# Small-disturbance Voltage Stability of OLTC & Decentralized Reactive Power Droop Control

Kilian Dallmer-Zerbe, Daniele Berardo, Ammar Salman, Bernhard Wille-Haussmann
Division Electrical Energy Systems EES
Fraunhofer Institute for Solar Energy Systems ISE
Freiburg, Germany
kilian.dallmer-zerbe@ise.fraunhofer.de

***Abstract*—Increasing installation of decentralized generators in distribution grids can cause critical grid states. In case of critical nodal voltages on-load tap-changers (OLTC) and reactive power control based on nodal voltage, Q(V), are regarded as comparably cheap solutions to delay or even to replace distribution grid reinforcement. Since both control schemes are based on nodal voltages and usually share no communication infrastructure, local oscillations between controllers are possible. This publication investigates small-disturbance voltage stability and potential local plant control oscillations of OLTC and multiple Q(V) in a rural low voltage feeder via dynamic RMS analysis.**

***Index Terms*--droop control, on-load tap-changer, reactive power control, stability.**

## I. Chance & Challenge of Decentralized Control

In recent years the number of decentralized generators in low and medium voltage level of distribution grids has increased. Nowadays these generators influence system states such as nodal voltages especially in rural or suburban grids significantly. Due to this reason decentralized generators are obliged to provide reactive power control, if the distribution system operator demands it. Decentralized reactive power control is used as a comparably cheap option to influence critical voltage levels in locations, where potential additional reactive current flows can be integrated. Thereby reactive power provision based on local voltages Q(V) is considered as most efficient way to influence voltage levels only at critical times [4]. Q(V) control includes a first order lag (PT1) element.

Another option of voltage control is the on-load tap-changer (OLTC), which can change its taps stepwise under load based on local grid states. This technology decouples low and medium voltage levels and enables a higher voltage band and potentially more decentralized generators within low voltage grids without conventional grid reinforcement. Usual control algorithms of OLTCs consist of a three point control with a dead band which is damped or delayed by a proportional integrator (PI) part [3]. The discontinuous step operations can oscillate with the continuous decentralized droop Q(V) control.

978-1-4673-8463-6/16/$31.00 ©2016 IEEE
Gefördert durch:
Bundesministerium für Wirtschaft und Energie
aufgrund eines Beschlusses des Deutschen Bundestages

**The research leading to these results was developed within the "Green Access" project financed by the German Ministry of Economics and Energy (BMWi).**

Another possibility is the interference of multiple Q(V) controllers.

Dynamic simulations of reactive power controllers were presented in [5, 7]. Multiple Q(V) controllers were tested in parallel configuration within a rural feeder representation in [8]. This publication executes a sensitivity analysis of parameterizations of multiple Q(V) controllers and in a second step of multiple Q(V) controllers as well as an OLTC. Thereby the focus lies on small disturbance voltage stability according to [6] on rural low voltage feeders. The shape of the Q(V)-droop is varied, especially the slope between maximal an minimal reactive power provision. Additionally tag elements of each controller are varied to check decoupling of different controls within time scale. Dynamic simulation of a rural low voltage feeder is implemented in DIgSILENT PowerFactory.

## II. Controller Models

All controllers are parameterized to keep the nodal voltages within the low voltage grid between -4% according to [1] and +3% according to [2].

### *A. Reactive Power Droop Control*

The reactive power provision is controlled based on local nodal voltage measurement. Additionally, control algorithms are in this case either dependent on current active power $P_{in}$, namely tanφ(V) or independent defined as Q(V).

#### *1) Dependent on Active Power & Nodal Voltage: tanφ(V)*

The reactive power provision is calculated via (1) based on $tan\varphi$ and nodal voltage $V$. The $tan\varphi$-value is extracted based on the current voltage from defined droops as depicted in Figure 1.

$$Q_{out} = tan\varphi(V) \cdot P_{in} \quad (1)$$

The maximal reactive power provision is limited via $cos\varphi$ of 0.9 as specified in (2)

$$\max\left(tan\varphi(V)\right) = \tan\left(acos(cos\varphi)\right) = \tan\left(acos(0.9)\right) \quad (2)$$

Figure 1 shows all used droops. The deadband is increased by 1%-steps of the nodal voltage and yields slopes over 0.5% up to 3.0% of the nodal voltage.

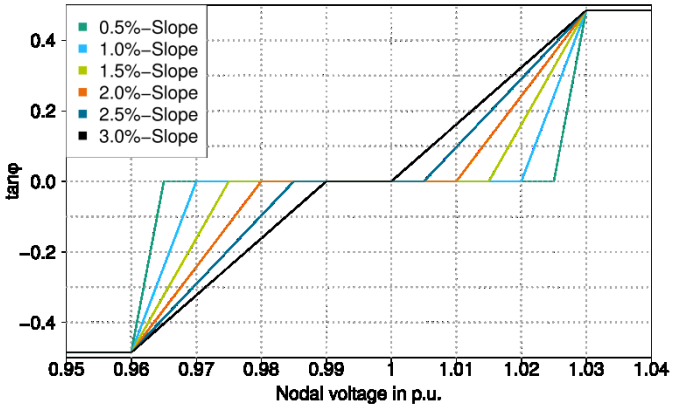


**Figure 1: Droop for nodal voltage and active power dependent reactive power provision tanφ(V)**

Figure 2 shows the control structure of the tanφ(V) controller. Input voltage is damped by a PT1 part which is parameterized via external $\tau$. Its output is fed into the droop block. The droop block is parameterized by external values of the dead band $\Delta V_{nom}$ as defined in (4). Its output $tan\varphi_{out}$ is multiplied with current active power according to (1) to calculate $Q_{out}$. Damped voltage $V$ is used to calculate a reactive current from reactive power $Q_{out}$.

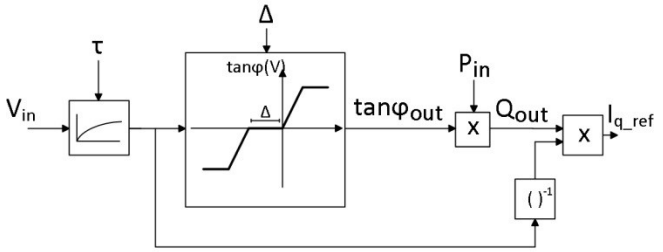


**Figure 2: Control structure of tanφ(V) controller**

*2) Only dependent on Nodal Voltage: Q(V)*

The Q(V)-controller provides reactive power independent of the current active power. Since all variables are normalized and in p.u., Q(V)-droops and tanφ(V)-droops look alike apart from the Y-axis label. Figure 1 can be used with alternative Y-axis of "Q in p.u". Applying Q(V)-droops solves not only grid problems initiated by the plant itself. Therefore PV plants could solve nodal voltage problems caused by electric vehicles even at times with no sunshine and hence no active power provision by the PV unit.

Figure 3 shows the control structure of the Q(V) controller, which is a simplified version of Figure 2. Reactive power is directly calculated from nodal voltage without active power dependency.

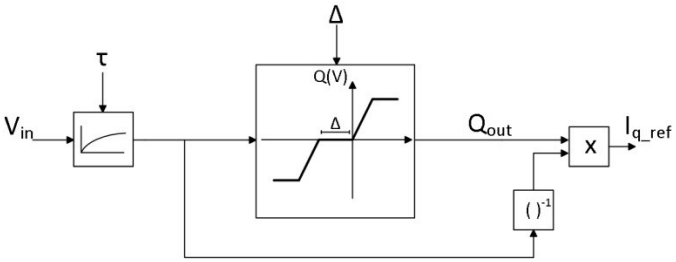


**Figure 3: Control structure of Q(V) controller**

*B. On-Load Tap-Changer (OLTC)*

The control structure of the OLTC is visualized in Figure 4 and features two tree point controller for fast switching and normal switching procedure. Voltage $V_{act}$ is measured at the low voltage bus bar. Its difference towards nominal voltage $V_{nom}$ is normalized by $\Delta V_{nom}$ and input to both thee point controllers.

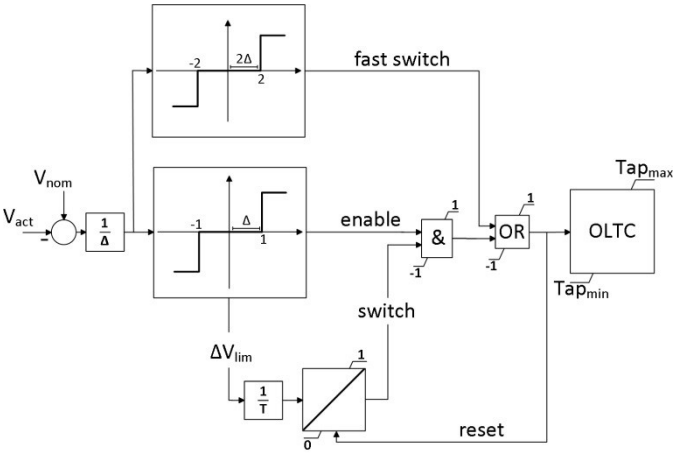


**Figure 4: Control structure of tap changer within OLTC**

OLTC switching is damped via integrator as long as the current nodal voltage $V_{act}$ is below twice $\Delta V_{nom}$ as marked in Figure 5. $\Delta V_{nom}$ is defined in (4) as difference of $V_{lim}$ and nominal voltage $V_{nom}$. If the integrator is active differences towards $V_{lim}$ as defined in (3) are integrated after normalization by $T$. The state of the integrator is decreased if $V_{act}$ drops below $V_{lim}$. The limit to trigger a tap change is set to $T$ of 60s.

$$\Delta V_{lim} = V_{act} - V_{lim} \quad (3)$$

$$\Delta V_{nom} = V_{lim} - V_{nom} \quad (4)$$

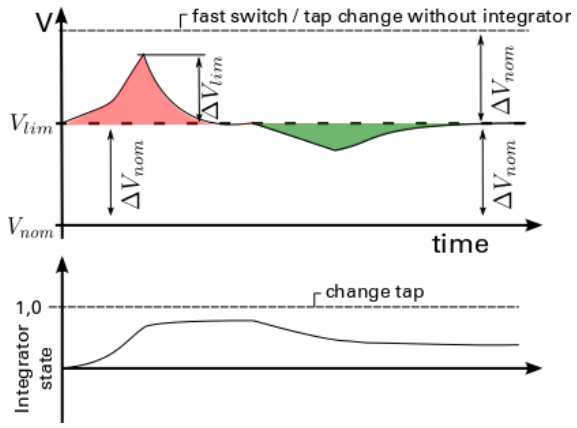


**Figure 5: Schematic of OLTC switch damping**

## III. Method for Interference Analysis

### A. Input Signals for Load Flow Calculation

Simulations are carried out with two different input signals via step and square function as visualized in Figure 6: Input signals for PV units. Whereas the square function jumps directly towards maximal nominal active power, the step function uses 20% active power steps. Each step is held for 80 seconds. Time resolution is due to automatic step size adaption between 20ms and 80ms.

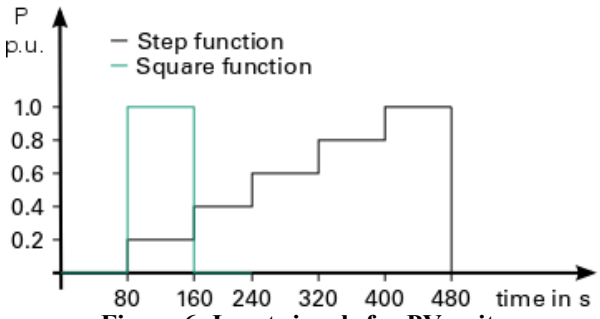


**Figure 6: Input signals for PV units**

### B. Sensitivity Analysis of Controller Parameters

Sensitivity analysis of controller parameters is structured into three parts:

#### 1) Deadband or Droop Slope

Deadband or slope of the droop are varied between slopes of 0.5% of nominal voltage and 3% as depicted in Figure 1. If the deadband is large (or droop slope over smaller voltage range), overall reactive energy is reduced. At the same time smaller deadbands enable more PV units to solve voltage problems in parallel.

#### 2) Tag Element

The tag element is used to integrate active power variation caused by clouds. Therefore the input signal is shifted between PV units by 15s according to [8].

#### 3) First Order Lag (PT1)

The first order lag element (PT1) is parameterized via time constant $\tau$ between 0 and 5 seconds. If PT1 is set to 0 second, PT1 is bypassed. The bigger $\tau$ is, the longer PV units need to react on a voltage change.

## IV. Distribution Grid Model

Within this publication a comparably small distribution grid feeder as shown in Figure 7 is used to test dynamic models of PV reactive controller and On-Load Tap-Changer. The PV units are distributed either at different nodes ("diff.") or combined at the same node at the end of the feeder ("same"). The active power per PV unit is varied between 9, 18 and 27kW in three separated simulation runs. Additionally active controllers, PT1 parameters and the tag element are varied as assembled in Table 1. The analysis is limited to the low voltage level. Voltage changes caused within the medium voltage level are not modeled. Cables are modeled as N2XRY 3x150sm type (R=0.141Ω, X=0.078Ω, L=0,258mH) between each node.

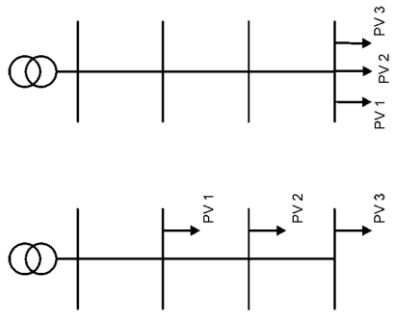


**Figure 7: Topologies of distribution feeder according to [8]**

**Table 1: Scenario structure of sensitivity analysis**

| # | PV units Pos. | P per PV in kW | $\tau$ of PT1 in s | Slope range in % | With clouds | Applied controller models | | |
|---|---|---|---|---|---|---|---|---|
| | | | | | | *tanφ(V)* | *Q(V)* | *OLTC* |
| 1 | same | 9, 18, 27 | 1, 2, 3, 4, 5 | 0.5, 1.0, 1.5, 2.0, 2.5, 3.0 | +/- | + | - | - |
| 2 | diff. | 9, 18, 27 | 1, 2, 3, 4, 5 | 0.5, 1.0, 1.5, 2.0, 2.5, 3.0 | +/- | - | + | - |
| 3 | same | 9, 18, 27 | 1, 2, 3, 4, 5 | 0.5, 1.0, 1.5, 2.0, 2.5, 3.0 | +/- | + | - | + |
| 4 | diff. | 9, 18, 27 | 1, 2, 3, 4, 5 | 0.5, 1.0, 1.5, 2.0, 2.5, 3.0 | +/- | - | + | + |

## V. Results of Interference Analysis

The interference analysis is structured into examples of the interference and results per square and step function. OLTC scenarios 3 and 4 did not yield additional interferences because the measurement of the OLTC at the busbar in combination with switch damping led to no changes of taps within the scenarios. Therefore scenario 3 and 4 are omitted within following results paragraphs. All controller interferences were solved once PT1 part was active with a $\tau$ starting from 2 second. Following discussions are therefore limited to a range of 2 seconds of $\tau$.

### A. Examples of Interference

Three different types of interference of the decentralized controllers were observed and are described in following paragraphs. These oscillations are differentiated based on the amplitude of the oscillation into decreasing, stable and fluctuating amplitude interferences. Increasing amplitude interference was not observed due to the fact that no controller uses amplification. Interferences are differentiated based on a comparison of voltage at the connection point of the PV unit (V before PT1) and voltage after PT1 part because nodal voltage is affected from active and reactive power provision of all controllers.

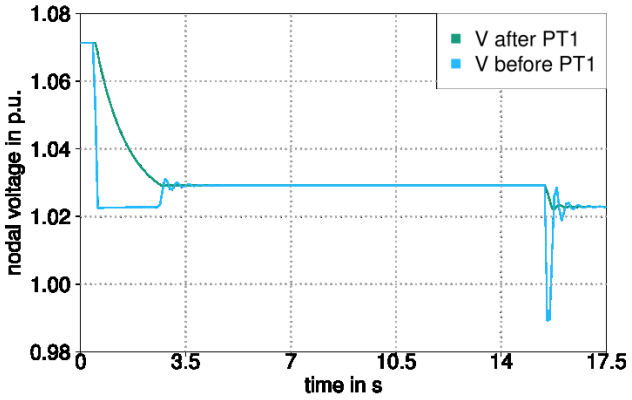


**Figure 8: Example for decreasing amplitude interference of Q(V) controller at PV unit with 27kVA and clouds**

#### 1) Decreasing Amplitude

Figure 8 shows two decreasing amplitude interferences at 3 and 16s for nodal voltage before and after PT1 part. The amplitude decreases towards a stable state. The figure illustrates also advantage and disadvantage of the PT1 part. At 1 second the voltage before PT1 part drops rapidly. The change is damped by the PT1 part leading to comparably smooth controller reaction. The disadvantage of the PT1 part is that fast changes as at second 16 are not controlled directly but with a time shift. Thereby fast critical system states cannot be controlled. Interferences with a decreasing amplitude or convergent behavior are interpreted as uncritical and stable in following results plots.

#### 2) Stable Amplitude

Interferences with a stable amplitude can be observed in Figure 9 between second 36 and 72. The PT1 part damps the amplitude of the interference efficiently. Stable amplitude interferences are regarded as unstable control scenarios because they are not converging towards steady state. An example can be two controllers that constantly switch reactive power provision due to effects of the other controller.

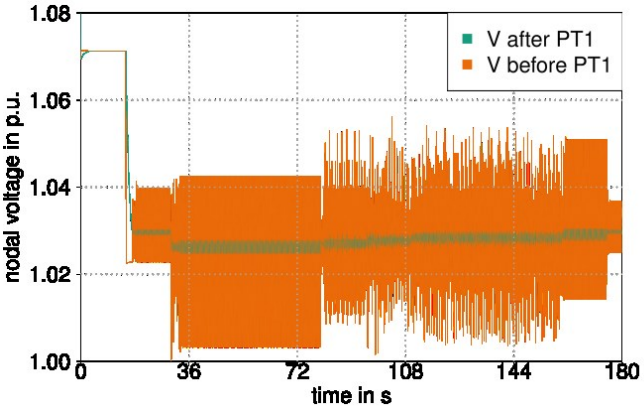


**Figure 9: Example for stable and fluctuating amplitude interference of Q(V) controller with clouds**

#### 3) Fluctuating Amplitude

Stable amplitude interference is changing towards fluctuating amplitude interferences starting from second 80 in Figure 9. This case can be observed if three controllers operate within their slopes of the droop. Fluctuating amplitude interference was only observed at activated PT1 part with $\tau$ above 1 second.

### B. Square Function as Input

Figure 10 and Figure 11 visualize the results of the sensitivity analysis using a square function (Figure 6) as input signal of the PV units. Each figure is structured by controller type (Q(V) a,c or tanφ(V) b,d) and clouds (with a,b or without c,d). One matrix shows the results of the sensitivity analysis of slope and $\tau$ of the PT1 part. Instability is color coded based on the number of unstable power scenarios. If a square is black power scenario (9, 18 and 27kW) yield instable or non-convergent results. If any scenario is stable the active power scenario (9, 18 or 27 kW) is printed on the results cell.

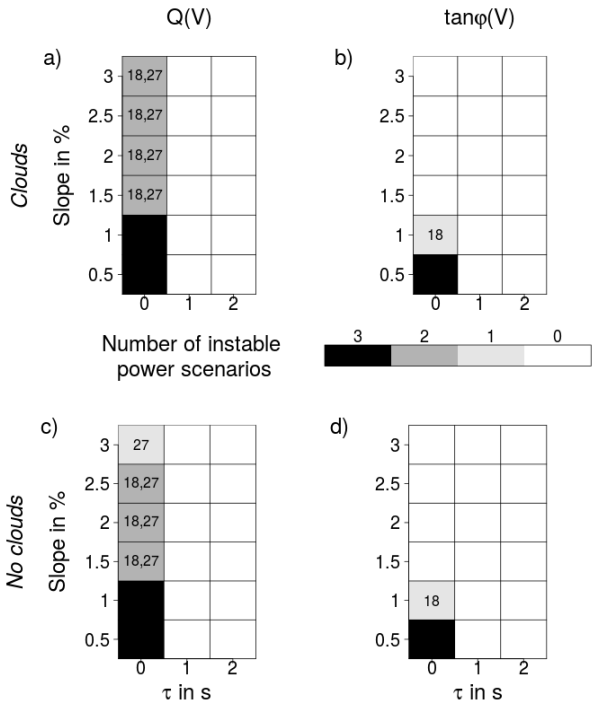


**Figure 10: Square function: PV units at different positions. Numbers within cells indicate active power scenarios**

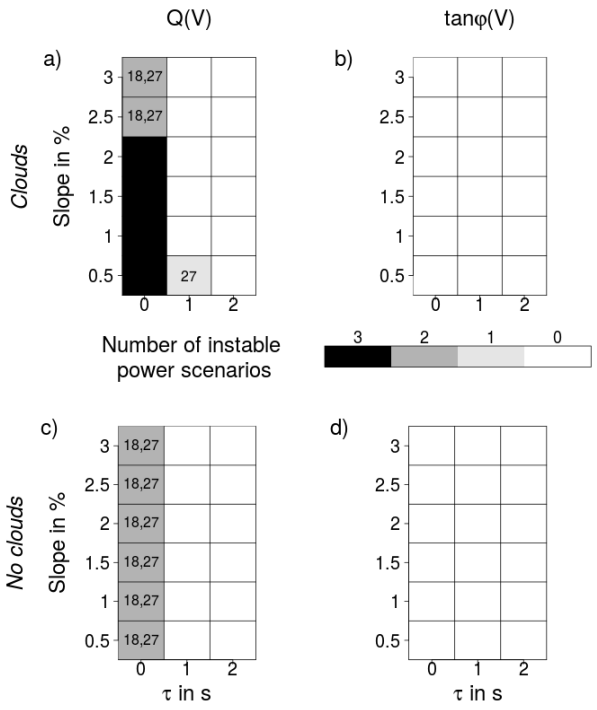


**Figure 11: Square function: PV units at same position. Numbers within cells indicate active power scenarios**

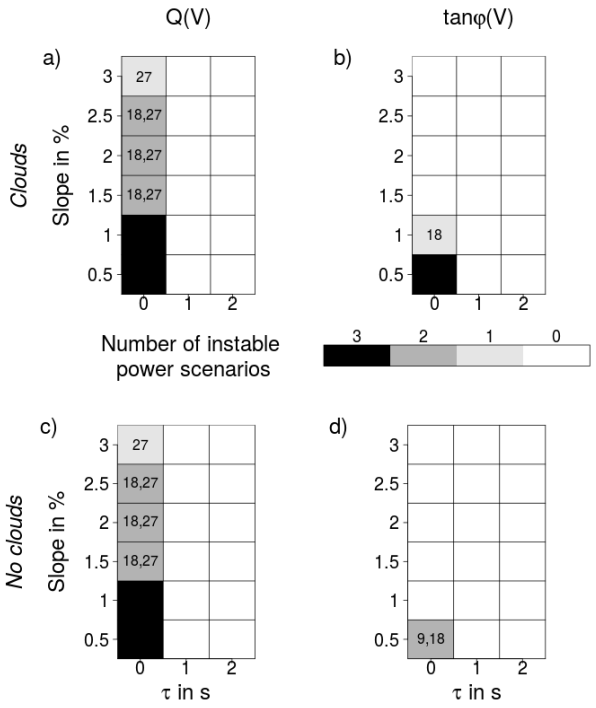


**Figure 12: Step function: PV units at different positions. Numbers within cells indicate active power scenarios**

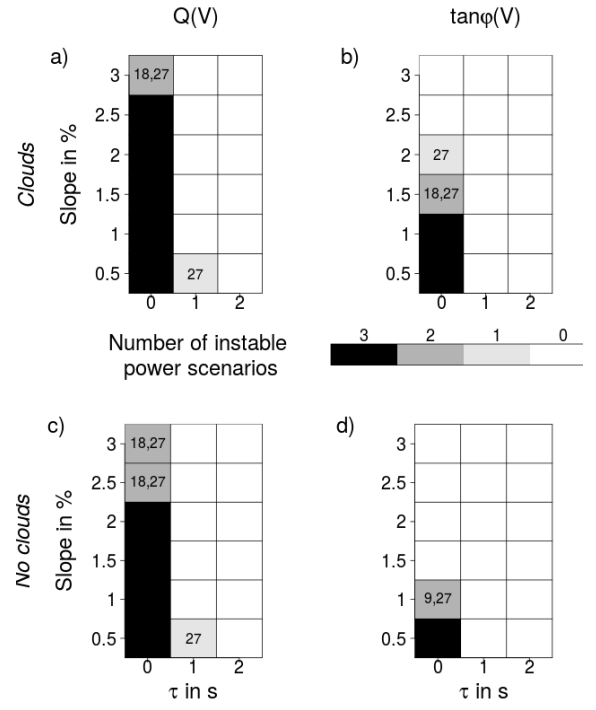


**Figure 13: Step function: PV units at same position. Numbers within cells indicate active power scenarios**

*1) Multiple Q(V) Controllers*

If PV units are distributed over the feeder (Figure 10a,c), critical scenarios decrease in comparison to scenarios with all PV units at the same node (Figure 11a,c). With increasing slope ranges the controller operates more stably at lower powers of the individual PV unit. If all Q(V) controllers are connected at the same position, the PT1 element ($\tau$ of 1s) does not prevent all instabilities (Figure 11a). Without clouds and all PV units at the same node (Figure 11c) the smallest power scenario is in every parameter combination stable.

*2) Multiple tanφ(V) Controllers*

Tanφ(V) controllers show less instability in comparison to Q(V) controllers. Starting from slopes over 1.5% of the nominal voltage and higher all combinations are stable (Figure 10 b,d). Tanφ(V) controller are stable even with clouds if they are positioned at the same node (Figure 11 b,d).

### C. Step Function as Input

Figure 12 and Figure 13 visualize the results of the sensitivity analysis using a step function (Figure 6) as input signal of the PV units. In comparison to results with square function input, the number of unstable scenarios is increased. Differences for clouding decrease for step function input in comparison to square function input.

*1) Multiple Q(V) Controllers*

There are no differences for clouding if all PV units are distributed over the feeder (Figure 12 a,c) in contrary to all PV units at the same position (Figure 13 a,c). With rising power of the individual PV units, instabilities increase. In comparison to tanφ(V) controllers, Q(V) controllers operate less stably.

*2) Multiple tanφ(V) Controllers*

For tanφ(V) controllers clouding increases instabilities regardless of the position of the PV units (Figure 12 b,d and Figure 13 b,d). Tanφ(V) controller operate stably if the droop slope is stretched over at least 2.5% of the nominal voltage.

### D. Overall Trends

Within the presented sensitivity analysis several overall trends were found:

1. The larger the influence of the PV units is on the nodal voltages within a grid, the more interference and oscillation between each decentralized controller was observed.
2. Tanφ(V) controllers interfere less due to dependency and therefore damping of the reactive power by the active power provision of the PV units.
3. Clouds or tag elements increase the number of instabilities, because steady state is reached later.
4. Step function input leads to more unstable scenarios.
5. Droop slopes over small ranges of the nominal voltage increase the number of instable scenarios.
6. PT1 part reduces instabilities rapidly to no observed cases at $\tau$ of 2 seconds.

## VI. Discussion & Outlook

Within this publication a sensitivity analysis with different controller types, generator positions and controller parameters was carried out to identify potentially instable parameter sets of multiple decentralized reactive power controllers in a first step. And within a second step with additional OLTCs. Since results with an additional OLTC do not deviate from results without it, they were not reported. In future research the effect of the reactive power controllers on the nodal voltages of the low voltage side will be increased to investigate interference of OLTC and reactive power controllers.

Several overall trends could be identified based on this sensitivity analysis. In future publications these trends will be tested for different low voltage grids. Furthermore, instable scenarios are going to be tested and validated in laboratory environment.

## VII. Acknowledgement

This research was developed within the project “Green Access” and has received Federal Ministry for the Environment, Nature Conservation, Building and Nuclear Safety under grant agreement No 03ET7534.

## VIII. References

[1] EN 50160 Voltage characteristics of electricity supplied by public distribution systems. 2010.

[2] VDE-AR-N 4105 Anwendungsregel:2011-08 Erzeugungsanlagen am Niederspannungsnetz.

[3] A. Becker, editor. *Netzausbauvarianten in Niederspannungsverteilnetzen: Regelbare Ortsnetztransformatoren in Konkurrenz zu konventionellen Netzausbaumaßnahmen ; eine technische und wirtschaftliche Betrachtung*, volume 20 of *Schriftenreihe des Energie-Forschungszentrums Niedersachsen*. Cuvillier, Göttingen, 1. aufl edition, 2014.

[4] Kilian Dallmer-Zerbe, Wolfgang Biener, and Bernhard Wille-Haussmann. Reactive power control in low voltage distribution grids: Comparison of centralized and decentralized q(u)-controller designs based on probabilistic load flow. In *Security in Critical Infrastructures Today, Proceedings of International ETG-Congress 2013; Symposium 1:*, pages 1–6, Nov 2013.

[5] Matthias Kahl and Thomas Leibfried. Stabilitätsanalyse von stromrichterbetriebene Anlagen zur Blindleistungskompensation und deren Auslegung. In *VDE-Kongress 2012*. VDE VERLAG GmbH, 2012.

[6] P. Kundur, J. Paserba, V. Ajjarapu, G. Andersson, A. Bose, C. Canizares, N. Hatziargyriou, D. Hill, A. Stankovic, C. Taylor, T. Van Cutsem, and V. Vittal. Definition and classification of power system stability ieee/cigre joint task force on stability terms and definitions. *Power Systems, IEEE Transactions on*, 19(3):1387–1401, Aug 2004.

[7] Ravindra, H. and Faruque, M.O. and Schoder, K. and Steurer, M. and McLaren, P. and Meeker, R. Dynamic interactions between distribution network voltage regulators for large and distributed PV plants. In *Transmission and Distribution Conference and Exposition (T D), 2012 IEEE PES*, pages 1–8, May 2012.

[8] R. Witzmann. *Studie Q(U)*. Technische Universität München, 2012.